Int. J. Heat Mass Transfer. Vol. 17, pp. 1549–1557. Pergamon Press 1974. Printed in Great Britain

FORCED CONVECTIVE HEAT AND MASS TRANSFER FROM A FALLING FILM TO A LAMINAR EXTERNAL BOUNDARY LAYER

VIJAY CHANDRA* and C. WILLIAM SAVERY†
Mechanical Engineering and Mechanics Department, Drexel University, Philadelphia, Pennsylvania 19104, U.S.A.

(*Received* 15 *September* 1973 *and in revised form* 24 *January* 1974)

Abstract—Simultaneous momentum, heat- and mass-transfer rates from a vertical falling liquid film to an upward flow of gas are reported. The gas forms an external boundary layer along the liquid film. In all cases dimensionless transport rates were determined from property gradients measured at the inner edge of the boundary layer. The velocity, temperature and concentration profiles were measured using hot wire anemometric, thermocouple probe and isokinetic sampling with gas chromatographic analysis techniques. Particular numerical and integral solutions to the boundary-layer equations are in good agreement with the data.

NOMENCLATURE

a, coefficient in concentration boundary condition [kg mole];
a', coefficient in temperature boundary condition [K];
b, coefficient in concentration boundary condition [kg mole/m];
b', coefficient in temperature boundary condition [K/m];
c, molar density of mixture [kg mole/m^3];
$\mathscr{D}_{AB}$, coefficient of binary diffusion coefficient (*iso*propyl alcohol vapors in air) [m^2/s];
f, friction factor at liquid–air interface;
h_x, heat-transfer coefficient [W/m^2 K];
k_x, mass-transfer coefficient [kg/mole/m^{2}s];
m, average liquid flow rate per unit width in the film [kg/m s];
Nu, Nusselt number;
p, see equation (14);
Pr, Prandtl number;
q, heat flux at the liquid vapor interface [W/m^2 K] also see equation (14);
r, $= 1 - \left(\frac{\xi}{x}\right)^{3/4}$, see equation (13);
Re, Reynolds number;
Sc, Schmidt number;
Sh, Sherwood number;
T, temperature (K);
u, x component of velocity [m/s];
v, y component of velocity [m/s];
$W_{A,o}$, molar flux of A at boundary [kg mole/m^{2}s];
x, distance from leading edge [m];
x_A, mole fraction of vaporizing species;
y, distance from film surface [m];
Z, dummy variable, see equation (14);
α, thermal diffusivity of vapor air mixture [m^2/s];
β_r, incomplete beta function;
δ, velocity boundary layer thickness [m];
Δ, temperature boundary layer thickness [m];
ΔT_o, step change in temperature boundary condition [K];
$\Delta x_{A,o}$, step change in concentration boundary condition;
θ, dimensionless temperature;
ξ, unwet starting length, running variable in equation (26) [m];
ν, kinematic viscosity of vapor air mixture [m^2/s];
τ, shear stress [N/m^2];
μ, viscosity of vapor air mixture [Ns/m^2];
ρ, density of vapor air mixture [kg/m^3];
μ_1, viscosity of film liquid [Ns/m^2];
λ, thermal conductivity of vapor air mixture [W/m K].

Subscripts

x, at a distance from leading edge;
o, at liquid–gas interface;
i, ith ($i = 1, 2, \ldots, n$);

*Research Assistant.
†Assistant Professor, to whom correspondence should be directed.

∞, at free stream;
n, number of finite steps in boundary condition;
l, pertaining to liquid film;
A, pertaining to vaporizing species (*iso*propyl alcohol).

INTRODUCTION

FEW EXPERIMENTAL data exist for heat and mass transfer from liquid films to external flows for non-uniform temperature and concentration boundary conditions. These boundary conditions exist in the entrance region of film type packing in counter flow cooling towers and wetted wall gas absorption columns. Thus an apparatus of similar geometry was designed to study the heat- and mass-transfer phenomena. A technique which allows measurements of velocity, temperature and concentration profiles within a two dimensional boundary layer has been developed, and hence, dimensionless transport coefficients can be obtained. These coefficients have been measured for *iso*propyl alcohol vaporizing from a falling film into an upward forced flow of air at laboratory conditions, and comparisons with laminar boundary-layer theory results have been made.

Several studies of transport phenomena in systems where a moving interface exists between a liquid and vapor phase have been reported [1–5]. Pike [1] obtained pressure gradients and velocity profiles for fully developed turbulent flow for the co-current flow of a gas and liquid film in a rectangular duct. Isenberg and Gutfinger [2] analyzed the heat transfer to a falling vertical film whose thickness and surface temperature are changing with time. Mass-transfer measurements have been reported for internal flows with moving liquid–vapor interfaces [3, 4]. In a theoretical study Howard and Lightfoot [5] extended the surface-stretch mass-transfer model to the case of gas absorption into laminar rippling films.

The studies of Byers and King [3] and Barton and Trass [6] are noteworthy because of their reported concentration profile measurements. Byers and King used sub-local, constant velocity sampling by means of a probe traversing the fully developed gas phase of a two-phase flow in a horizontal rectangular channel. Barton and Trass developed an optical ultraviolet absorption technique for measuring concentration profiles in an external vertical boundary layer with a stationary vaporizing solid phase wall.

ANALYSIS

Following are the basic well known constant property boundary-layer equations for a flat plate [7].

$$\frac{\partial u}{\partial x}+\frac{\partial v}{\partial y}=0 \tag{1}$$

$$u\frac{\partial u}{\partial x}+v\frac{\partial u}{\partial y}=\nu\frac{\partial^2 u}{\partial y^2} \tag{2}$$

$$u\frac{\partial T}{\partial x}+v\frac{\partial T}{\partial y}=\alpha\frac{\partial^2 T}{\partial y^2} \tag{3}$$

$$u\frac{\partial x_A}{\partial x}+v\frac{\partial x_A}{\partial y}=\mathscr{D}_{AB}\frac{\partial^2 x_A}{\partial y^2} \tag{4}$$

where,

T = temperature;
x_A = mole fraction of vapor;
α = thermal diffusivity of the mixture;
$\mathscr{D}_{AB}$ = diffusion coefficient of vapor diffusing into air;
ν = kinematic viscosity of the vapor mixture.

No chemical reactions, external force fields and viscous dissipation are assumed to exist in applying equations (1)–(4). Equations (1) and (2) have been solved exactly by Blasius for zero velocity at the wall and the results are tabulated in [8].

The expression for friction factor which is defined as

$$f_x=\frac{\tau_{x,o}}{\frac{1}{2}\rho u_\infty^2} \tag{5}$$

is given by

$$f_x=\frac{0{\cdot}664}{Re_x^{1/2}} \tag{6}$$

$$Re_x=\frac{u_\infty x}{\nu} \tag{7}$$

where

$\tau_{x,o}$ = shear stress at the wall at location x;
u_∞ = free stream velocity.

In order to get expressions for heat- and mass-transfer coefficients the groups of equations (1)–(3) and (1), (2) and (4) have to be solved simultaneously. The exact solutions can not be obtained for the inhomogeneous boundary conditions. Hence these equations have been solved approximately employing integral techniques [9].

If the boundary conditions are as follows

$$u(x,o)=0,\quad v(x,o)=0 \tag{8}$$

$$\begin{aligned} T(x,o)&=T_o=T_\infty; && 0\leqq x\leqq\xi\\ &=a'+b'x; && x\geqq\xi \end{aligned} \tag{9}$$

and

$$\begin{aligned} x_A(x,o)&=x_{A,o}=x_{A,\infty}; && o\leqq x\leqq\xi\\ &=a+bx; && x\geqq\xi \end{aligned} \tag{10}$$

and if the free stream conditions are constant then the

expressions for the local Nusselt and Sherwood numbers are*

$$Nu_x = \frac{0{\cdot}332 P_r^{1/3} Re_x^{1/2}}{T_o - T_\infty}\left[\frac{\Delta T_o}{r^{1/3}} + 4/3 b' x \beta_r(\tfrac{2}{3}, \tfrac{4}{3})\right] \quad (11)$$

$$Sh_x = \frac{0{\cdot}332 Sc^{1/3} Re_x^{1/2}}{x_{A,o} - x_{A,\infty}}\left[\frac{\Delta x_{A,o}}{r^{1/3}} + 4/3 b x \beta_r(\tfrac{2}{3}, \tfrac{4}{3})\right] \quad (12)$$

where

$$r = 1 - \left(\frac{\xi}{x}\right)^{3/4} \quad (13)$$

$$\beta_r(p, q) = \int_0^r Z^{p-1}(1-Z)^{q-1}\,dz \quad (14)$$

ΔT_o = step in temperature boundary condition at $x = \xi$

$$= a' + b'\xi - T_\infty, \quad (15)$$

$\Delta x_{A,o}$ = step in concentration boundary condition at $x = \xi$

$$= a + b\xi \qquad (\text{since } x_{A,\infty} = 0), \quad (16)$$

$\beta(p, q)$ is the beta function.

In addition particular numerical solutions to the energy and species continuity equations, equations (3) and (4), were obtained for the boundary conditions measured at the wall. The Crank Nicolson implicit technique was employed [10]. The simultaneous difference equations were then solved by the Gaussian elimination method. The boundary condition of velocity at the liquid gas interphase was assumed to be zero because the film was ripple-free and the film surface velocity was only 0·018 m/s which was only 2 per cent of the free stream velocity. Further justification is stated in the "Results" Section.

EXPERIMENTAL TECHNIQUES

The schematic arrangement of the experimental setup is shown in Fig. 1. The test section was 7·0 × 14·5 cm and 49·8 cm in the flow direction. The air flow rate is controlled by the pressure regulator. The air passes through a subdivided divergent nozzle, a screened calming section and then into a convergent nozzle which produces a uniform velocity profile at the entrance of the test section [11]. A film of *iso*propyl alcohol falls vertically down the left wall of the test section. *Iso*propyl alcohol was chosen because it has low surface tension and therefore a very thin film can be formed. The liquid which is stored in the top reservoir enters the distributor where it calms and is distributed along the width of the film. The liquid is collected near the bottom of the test section. The film thickness can be controlled by adjusting the entrance slit opening or by adjusting the liquid level in the distributor.

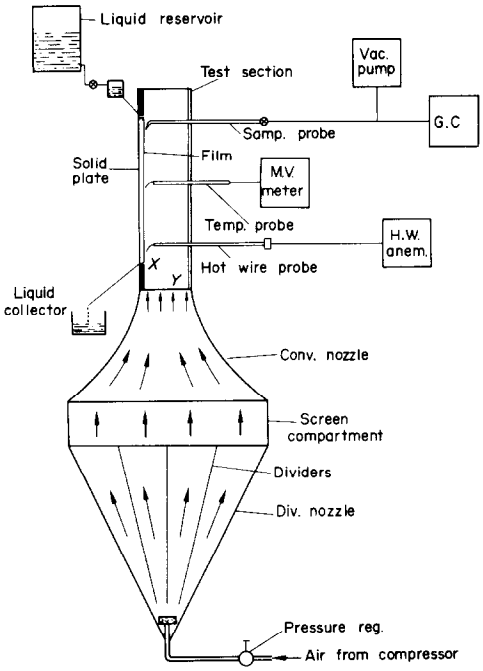

FIG. 1. Schematic arrangement of experiment.

Physically the experimental arrangement results in vaporization from a vertical falling film to an upward flowing stream of air. The air velocity is uniform at the leading edge of the starting length. At the end of the starting length the concentration and temperature boundary layers start developing simultaneously. The liquid which enters the falling film at ambient temperature cools down as it flows downward because of vaporization.

Velocity measurements

Velocities were measured with a flow corporation model 900 constant temperature hot wire anemometer equipped with a boundary-layer velocity probe. It was nec ssary to develop a method to calibrate the probe for velocities below 1 m/s. The arrangement which consisted of measuring the centerline discharge velocity from a long tube connected downstream of a calibrated gas meter is shown in Fig. 2 [12]. For laminar flow in the tube the discharge velocity measured at the tube centerline was twice the average tube flow velocity determined from the metered flow. The velocity probe was mounted in a traversing mechanism and could be located at any one of four stations along the film. The probe was supported in tapped holes in the right hand wall of the test section shown in Fig. 1. Measured velocity profiles are shown in Fig. 3. The measured turbulence intensity in the flow direction at the test section inlet was 2·8 per cent.

*See Appendix A for algebraic details.

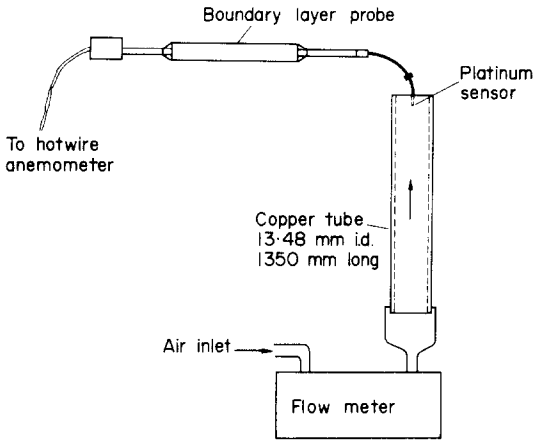

FIG. 2. Schematic arrangement for calibration of the hot wire anemometer probe.

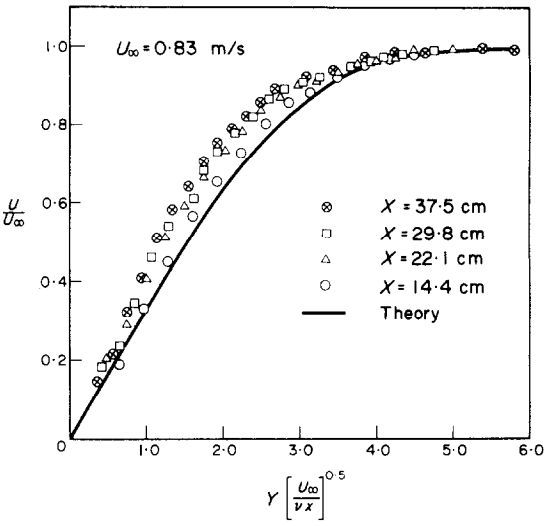

FIG. 3. Velocity profile.

Temperature measurements

Temperature profiles were measured by thermocouple probes. Considerable temperature probe development was necessary to reduce an erroneous temperature jump at the liquid film boundary-layer interface. The evolution of probe designs is shown in Fig. 4 where the probe was modified to reduce thermocouple lead wire conduction gains. The effect of reducing lead conduction gains in probe (a) by changing from Cu–Con to Cr–Con thermocouples and then by changing to the yoke configuration probe, probe (b), upon measured temperature profiles is shown in Fig. 5. The modified probe with 76 μm dia Cr–Con thermocouple lead wires was used for the reported measure-

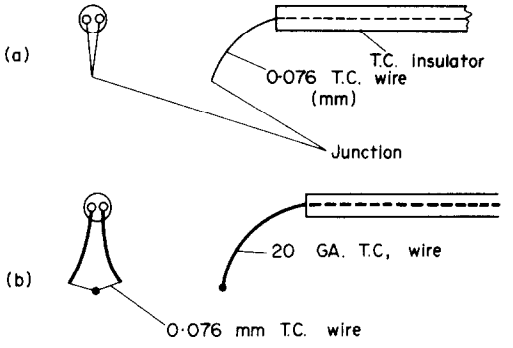

FIG. 4. Thermocouple probe designs: (a) original design: (b) modified design.

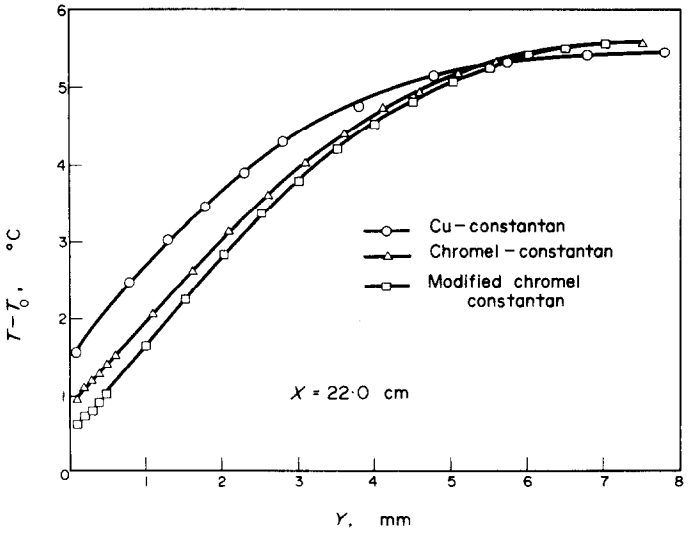

FIG. 5. Effect of probe design on temperature profile.

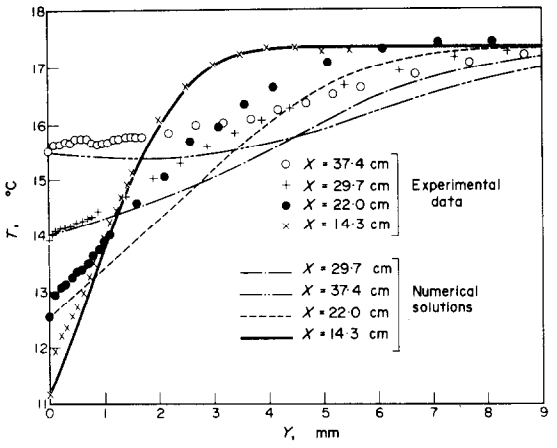

FIG. 6. Temperature profiles.

sampling loop was filled to the desired pressure the sample was injected into the gas chromatograph by the gas sampling valve.

Helium was used as a carrier gas. The flow rate in each column was maintained at 1 cm^3/s. A 0·635 cm dia 3·05 m long Porapak *Q* column was used to separate *iso*propyl alcohol from air. The columns were maintained at 138°C and the retention times of air and *iso*propyl alcohol were 0·5 and 7 min respectively. The concentration profiles are shown in Fig. 8. In order to reduce the running times of the experiments the profiles were measured only in the vicinity of the film. The concentration at the film surface was determined by assuming that the vapor is in equilibrium with liquid at the measured liquid temperature. Therefore, the partial pressure of vapor at the interface would be equal to its vapor pressure at that temperature.

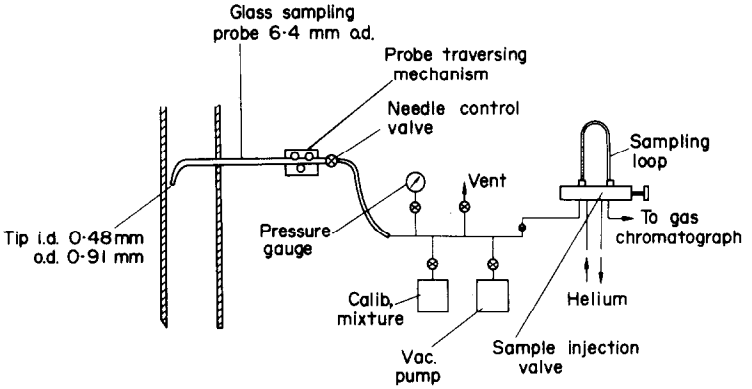

FIG. 7. Sampling manifold schematic.

ments. Temperature profiles measured within the boundary layer at the positions along the film are shown in Fig. 6 along with the numerical computer solutions.

Concentration measurements

The concentrations were measured by sampling the boundary layer and then injecting the sample in a Loenco model 2400 Graphmatic gas chromatograph equipped with a thermal conductivity detector. A diagram of the sampling manifold is shown in Fig. 7. The control valve was adjusted to perform *iso*-kinetic sampling with the probe, so that disturbances to the boundary-layer flow field are minimized and that the sample is drawn locally. The local sampling velocity which was measured previously by a hot wire anemometer is determined by timing the manifold filling process. The manifold which was initially evacuated and whose volume is known is filled to a predetermined pressure sufficiently below the test section to maintain critical flow during the sampling period. When the

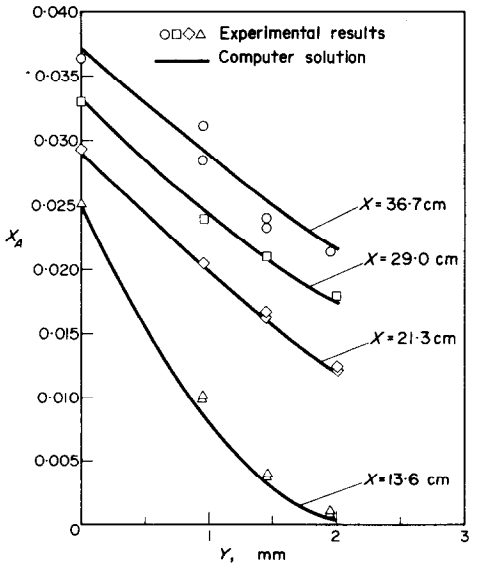

FIG. 8. Concentration profiles.

RESULTS

In this section the measured velocity, temperature and concentration profiles are presented and the transport coefficients derived from these measurements are compared with values calculated from boundary-layer theory. The measured liquid film vertical temperature distribution and the corresponding vapor phase concentration profile based upon thermodynamic liquid–vapor phase equilibrium are shown in Fig. 9. These measurements were used to specify the inhomogeneous boundary conditions of the energy and species continuity boundary-layer equations solved for comparison with the measured transport coefficients.

The velocity profiles measured at various positions along the wetted film are shown on Fig. 3. The discrepancy between the measured profiles and the exact flat plate boundary-layer results, although small, increases with the distance from the leading edge. This discrepancy is attributed to an increase in free stream velocity in the downstream direction. The measured free stream velocity increases from 0·82 to 0·845 m/s in the downstream direction; this is due to the three-dimensional effects of the bounded channel. Since the maximum boundary velocity at the film surface has been estimated to be 0·018 m/s which is only about 2 per cent of the free stream and in the opposite direction, it was assumed to be zero in numerical and approximate solutions of equation (1) through (4). This assumption can be further justified by the fact that the point of zero velocity is only $\delta/200$ away from the liquid vapor interphase. This expression was obtained using equation (4) of part II of reference [3]. Although this equation is strictly for flow between two parallel planes, it can be used for external flows if half the distance between parallel planes is replaced by the momentum boundary-layer thickness. Thus, in making an assumption of zero interface velocity, we have implicitly assumed that δ is off by 0·5 per cent and since Nu_x and Sh_x are approximately proportional to δ, the error in them will be of the order of 0·5 per cent. The film was also observed to be ripple-free. The film Reynolds number (m/μ_1) was 0·38. The ripples are present when Reynolds number exceeds 1 [7].

Equation (5) was used to determine the friction factor experimentally. The wall shear stress, $\tau_{x,o}$ was evaluated from equation (17).

$$\tau_{x,o} = \mu \left.\frac{\partial u}{\partial y}\right|_o . \tag{17}$$

The velocity gradient was obtained from measured velocity profiles. Table 1 shows a comparison between

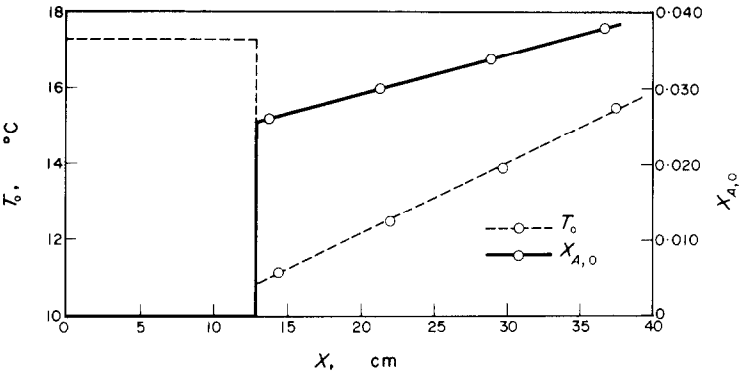

FIG. 9. Temperature and concentration boundary conditions.

Table 1. Comparison between measured and calculated transport coefficients

X (cm)	Theoretical		Experimental	Difference (%)
		Friction factor		
14·4	0·0075		0·0079	−5·1
22·1	0·0060		0·0072	−16·7
29·8	0·0052		0·0056	−7·1
37·5	0·0046		0·0051	−9·8
		Sherwood number		
13·6	94·2†	97·5*	90·6	+7·6
21·3	63·2	67·3	66·0	+2·5
29·0	81·9	71·9	84·0	−14·4
36·7	75·2	80·7	83·5	−3·4
		Nusselt number		
14·3	59·6†	59·7*	50·2	+18·9
22·0	38·0	37·9	44·8	−15·4
29·7	21·6	22·7	26·4	−14·6
37·4	−41·0	−17·4	36·5	High uncert.

*These values were calculated from particular solutions to boundary-layer equations obtained numerically.

†These values were calculated from approximate solutions using equations (11) and (12).

the experimentally and theoretically determined friction factors. The agreement is generally within about 10 per cent except for the comparison at station 2($x = 22{\cdot}1$ cm) where the values differ by 20 per cent.

The temperature profiles measured at the four positions along the film are shown in Fig. 6. The profiles become progressively flatter in the direction of the air flow with the difference between the free stream and the liquid film reaching a value less than 2°C at a position 37·4 cm from the leading edge of the plate.

Figure 9 shows the temperature boundary condition. $\xi(= 0{\cdot}128$ m) is the unwet starting length and the temperature of the wall is identical to the free stream temperature in this region. At $x = \xi$ there is a step in the temperature boundary condition because of the cold liquid film. The film surface temperature has been very closely approximated by a straight line. The Nusselt number, defined by the equation (18) can be computed as follows:

$$Nu_x = \frac{h_x x}{\lambda} \tag{18}$$

and since

$$q_o = -\lambda \left.\frac{\partial T}{\partial y}\right|_o = h_x(T_o - T_\infty) \tag{19}$$

therefore

$$Nu_x = -\frac{\left.\frac{\partial T}{\partial y}\right|_o x}{T_o - T_\infty} \tag{20}$$

and experimentally it can be determined by measuring the overall temperature difference and slope at the boundary. Measured and numerically obtained temperature profiles are shown in Fig. 6. The measured temperatures are in general higher than theoretical temperatures because the conduction in leads could not be completely eliminated. Since there is a jump in the measured temperature profiles at the boundary, the slope was measured by taking the difference between points located at 0·2 and 0·1 mm away from the film surface. In doing so it has been implicitly assumed that the error in the measured temperatures at $y = 0{\cdot}1$ mm and at $y = 0{\cdot}2$ mm is equal and it is reasonable.

Equation (11) was employed to calculate the Nusselt number corresponding to the four positions along the liquid film. The properties of air given in Table 2 were used for the calculation, since the vapor mixture never exceeded 4 per cent *iso*propyl alcohol. The predicted and measured Nusselt numbers are compared in Table 1. The error varies from −14 to 19 per cent for the first three stations. The error becomes very uncertain for station four because the terms within the brackets of equation (11) are opposite in sign and similar in absolute value.* The generally larger error in the Nusselt number is attributed to experimental uncertainty in the temperature measurement which is introduced into the measured results.

Table 2. Properties of the boundary layer

Diffusion coefficient, $\mathscr{D}_{AB}$	$0{\cdot}96 \times 10^{-5}$ m²/s
Thermal diffusivity, α	$0{\cdot}222 \times 10^{-4}$ m²/s
Kinematic viscosity, ν	$0{\cdot}157 \times 10^{-4}$ m²/s
Prandtl number, Pr	0·71
Schmidt number, Sc	1·64

Figure 9 also shows the concentration boundary condition. Here again there is an unwet starting length and the mole fraction of vapor is zero in this range. There is a step followed by a linear variation of mole fraction. Although the variation of vapor pressure with temperature is exponential, the concentration boundary condition can be approximated by a linear variation with length if the variation in the film surface temperature is small. It is worth mentioning that the temperature and concentration data were taken on different days and that on each day the system attained a different steady state depending on the room temperature. However, the temperatures needed to obtain concentration boundary conditions were measured on the same day that the concentration data was taken. Since the mole fraction of vapor everywhere is less than 4 per cent the use of equation (4), which is valid for low mass-transfer rates, is justified.

The mass flux rate from the surface of the film can be expressed as

$$W_{A,o}(x) = -c\mathscr{D}_{AB} \left.\frac{\partial x_A}{\partial y}\right|_o = k_x(x_{A,o} - x_{A,\infty}) \tag{21}$$

where

$$k_x = -\frac{c\mathscr{D}_{AB} \left.\frac{\partial x_A}{\partial y}\right|_o}{x_{A,o} - x_{A,\infty}}. \tag{22}$$

The Sherwood number is defined as

$$Sh_x = \frac{k_x x}{c\mathscr{D}_{AB}} = -\frac{\left.\frac{\partial x_A}{\partial y}\right|_o x}{x_{A,o} - x_{A,\infty}}. \tag{23}$$

Thus, experimentally it can be determined as with the Nusselt number by measuring the slope of the concentration profiles. Measured and numerically obtained concentration profiles are shown in Fig. 8. The agreement is quite good. The experimental and theoretical results as obtained by equation (12) are tabulated in Table 1. The agreement among the measured and calculated Sherwood numbers is quite good being generally within 8 per cent.

*And the Nusselt number is very strongly dependent on x and passes through zero in that region.

Acknowledgements—This work was partially sponsored by the Research Corporation in the form of a grant to the second author. The first author received support under the grant as a Graduate Research Assistant.

REFERENCES

1. J. G. Pike, Influence of a falling thin liquid film upon a co-currently flowing gas stream in a vertical duct, *Can. J. Chem. Engng* **43**, 267–270 (1965).
2. J. Isenberg and C. Gutfinger, Heat transfer to a draining film, *Int. J. Heat Mass Transfer* **16**, 505–512 (1973).
3. C. H. Byers and C. J. King, Gas–liquid mass transfer with a tangentially moving interface: Part 1 and 2, *A.I.Ch.E. Jl* **13**, 628–644 (1967).
4. M. W. Clark and C. J. King, Evaporation rates of volatile liquids in a laminar flow system, Part I and II, *A.I.Ch.E. Jl* **16**, 64–75 (1970).
5. D. W. Howard and E. N. Lightfoot, Mass transfer to falling films: Part 1. *A.I.Ch.E. Jl* **16**, 458–467 (1968).
6. H. J. Barton and O. Trass, Simultaneous heat and mass transfer through laminar boundary layers in combined forced and free convection, *Can. J. Chem. Engng* **47**, 20–29 (1969).
7. R. B. Bird, W. E. Stewart and E. N. Lightfoot, *Transport Phenomena*, pp. 41 and 609. John Wiley, New York (1960).
8. H. Schlichting, *Boundary-Layer Theory*, 6th Edn, p. 129. McGraw-Hill, New York (1968).
9. W. M. Kays, *Convective Heat and Mass Transfer*, pp. 215–218. McGraw-Hill, New York (1966).
10. G. D. Smith, *Numerical Solution of Partial Differential Equations*, pp. 17–21. Oxford University Press, New York (1965).
11. H. Mache and A. Hebra, Zur Messung der Verbrennungsgeschwindigkeit Explosiver Gasgemische, *Akad. Abteilung Wien* (IIa) **150**, 157–174 (1941).
12. P. Almquist and E. Legath, The hot-wire anemometer at low air velocities, *Disa Inform.* **2**, 3–4 (July 1965).

APPENDIX A

(a) *Approximate Solution to Energy Boundary-Layer Equation*

Let

$$\theta(\xi, x, y) = \frac{T_o - T}{T_o - T_\infty} \tag{A-1}$$

be the solution of a flat plate heat transfer problem with the boundary condition as shown in Fig. 10. Transposing the terms in (A-1)

$$T - T_\infty = (1-\theta)(T_o - T_\infty) \tag{A-2}$$

or

$$T - T_\infty = (1-\theta)(\Delta T_o) \tag{A-3}$$

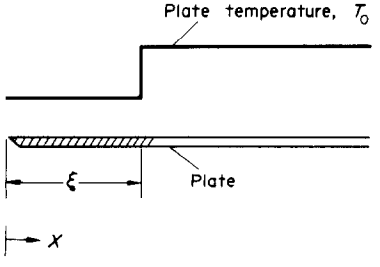

FIG. 10. Step function temperature boundary condition.

is obtained. If a problem has an arbitrarily specified boundary condition then its solution can be derived by superimposing the solution for each step and if the temperature variation at the boundary is continuous then this variation can be considered as a series of infinitesimal steps. This superimposing can be done because T appears only in first degree in the energy equation. In summing up the effect of each such step a running variable ξ is used to denote the location of a particular step [9]. Adding all the finite and infinitesimal steps the resultant solution can be written as

$$T - T_\infty = \int [1-\theta(\xi, x, y)]\,\mathrm{d}T_o + \sum_{i=1}^{n} [1-\theta(\xi_i, x, y)]\Delta T_{o,i}. \tag{A-4}$$

Since T_o is a function of ξ only

$$T - T_\infty = \int [1-\theta(\xi, x, y)]\left(\frac{\mathrm{d}T_o}{\mathrm{d}\xi}\right)\mathrm{d}\xi + \sum_{i=1}^{n} [1-\theta(\xi_i, x, y)]\Delta T_{o,i}. \tag{A-5}$$

But from reference [9]

$$\theta(\xi, x, y) = \frac{3}{2}\left(\frac{y}{\Delta}\right) - \frac{1}{2}\left(\frac{y}{\Delta}\right)^3 \tag{A-6}$$

where

$$\Delta = P_r^{-1/3}\left[1 - \left(\frac{\xi}{x}\right)^{3/4}\right]^{1/3}\delta \tag{A-7}$$

and

$$\delta = 4{\cdot}64\sqrt{\left(\frac{\nu x}{u_\infty}\right)}. \tag{A-8}$$

In the present investigation there is one finite step and a linear variation in boundary conditions, therefore substituting $n = 1$ and differentiating (A-5), following equation is obtained

$$\left.\frac{\partial T}{\partial y}\right|_o = -\frac{3\Delta T_o}{2\Delta} + \int_\xi^x \left(-\frac{3}{2}\frac{1}{\Delta}\right)\left(\frac{\mathrm{d}T_o}{\mathrm{d}\xi}\right)\mathrm{d}\xi. \tag{A-9}$$

Since

$$T_o = a' + b'x \qquad x \geqq \xi \tag{9}$$

$$\text{or } T_o = a' + b'\xi \tag{A-10}$$

$$\frac{\mathrm{d}T_o}{\mathrm{d}\xi} = b'. \tag{A-11}$$

Substituting (A-9) in (20)

$$Nu_x = \frac{0{\cdot}323 P_r^{1/3} Re_x^{1/2}}{T_o - T_\infty}\left[\frac{\Delta T_o}{r^{1/3}} + b'x\int_\xi^x \frac{\mathrm{d}\xi}{r^{1/3}}\right]. \tag{A-12}$$

Substituting $r = 1 - \left(\frac{\xi}{x}\right)^{3/4}$ into the integral, (13)

(A-13) is obtained

$$Nu_x = \frac{0{\cdot}323 P_r^{1/3} Re_x^{1/2}}{T_o - T_\infty}\left[\frac{\Delta T_o}{r^{1/3}} + \frac{4}{3}b'x\beta_r\left(\frac{2}{3}, \frac{4}{3}\right)\right]. \tag{A-13}$$

The coefficient 0·323 will be changed to 0·332 because the exact solution with no unheated starting length is [9]

$$Nu_x = 0{\cdot}332 P_r^{1/3} Re_x^{1/2}. \tag{A-14}$$

Similarly the expression for Sherwood number will be

$$Sh_x = \frac{0{\cdot}332 Sc^{1/3} Re_x^{1/2}}{x_{A,o} - x_{A,\xi}}\left[\frac{\Delta x_{A,o}}{r^{1/3}} + \frac{4}{3}bx\beta_r\left(\frac{2}{3}, \frac{4}{3}\right)\right]. \tag{12}$$

TRANSFERT DE CHALEUR ET DE MASSE PAR CONVECTION FORCEE ENTRE UN FILM TOMBANT ET UNE COUCHE LIMITE EXTERNE LAMINAIRE

Résumé—On considère les flux de transfert simultanés de chaleur, de masse et de quantité de mouvement entre un film liquide tombant et un écoulement ascendant de gaz. Le gaz forme une couche limite externe le long du film liquide. Dans tous les cas, les flux de transfert adimensionnels sont déterminés à partir des gradients mesurés au bord intérieur de la couche limite. Les profils de vitesse, de température et de concentration sont mesurés à l'aide de sondes anémométriques, de thermocouples et par des techniques d'analyse chromatographique. Des solutions particulières numériques et intégrales des équations de la couche limite sont en bon agrément avec les résultats expérimentaux.

WÄRME- UND STOFFÜBERGANG BEI ERZWUNGENER KONVEKTION VON EINEM RIESELFILM AN EINE LAMINARE ÄUßERE GRENZSCHICHT

Zusammenfassung—Es wird über die gleichzeitigen Impuls-, Wärme- und Stoffaustauschvorgänge zwischen einem senkrechten Rieselfilm und einem aufwärts strömenden Gas berichtet, wobei das Gas eine äußere Grenzschicht entlang des Rieselfilmes bildet. In allen Fällen wurden die dimensionslosen Transportraten aus den gemessenen Gradienten der Stoffeigenschaften an der Grenzschicht bestimmt. Die Geschwindigkeits-, Temperatur- und Konzentrationsverteilungen wurden mit Hilfe von Hitzdrahtanemometern, Thermoelementsonden und Gaschromatographen gemessen. Einzelne numerische und integrale Lösungen der Grenzschichtgleichungen zeigen eine gute Übereinstimmung mit den Meßwerten.

ВЫНУЖДЕННЫЙ КОНВЕКТИВНЫЙ ТЕПЛО- И МАССОПЕРЕНОС ОТ ПАДАЮЩЕЙ ПЛЕНКИ К ЛАМИНАРНОМУ ВНЕШНЕМУ ПОГРАНИЧНОМУ СЛОЮ

Аннотация — Приводятся данные по интенсивности одновременного переноса количества движения, тепла и массы от вертикальной падающей жидкой пленки к потоку газа, направленному вверх. Газ образует внешний пограничный слой вдоль жидкой пленки. Во всех случаях безразмерные скорости переноса определялись через градиенты рассматриваемой величины, измеряемые на внутренней границе пограничного слоя. Профили скорости, температуры и концентрации измерялись с помощью анемометров, термопар и изокинетического отбора проб с применением хроматографического анализа газа. Численные и интегральные решения уравнений пограничного слоя хорошо согласуются с полученными данными.